Water dynamics in *n*-propylene glycol aqueous solutions

S. Cerveny[a] and G. A. Schwartz
Donostia Internacional Physics Center, Paseo Manuel de Lardizabal 4, 20018 San Sebastián, Spain

A. Alegría
Unidad de Física de Materiales, Centro Mixto CSIC-UPV/EHU and Departamento de Física de Materiales, Facultad de Química, Universidad del País Vasco (UPV/EHU), Apartado 1072, 20018 San Sebastián, Spain

R. Bergman and J. Swenson
Department of Applied Physics, Chalmers University of Technology, 41296 Göteborg, Sweden

(Received 5 December 2005; accepted 29 March 2006; published online 15 May 2006)

The relaxation dynamics of dipropylene glycol and tripropylene glycol (*n*PG—$n=2,3$) water solutions on the *n*PG-rich side has been studied by broadband dielectric spectroscopy and differential scanning calorimetry in the temperature range of 130–280 K. Two relaxation processes are observed for all the hydration levels; the slower process (I) is related to the α relaxation of the solution whereas the faster one (II) is associated with the reorientation of water molecules in the mixture. Dielectric data for process (II) at temperatures between 150 and 200 K indicate the existence of a critical water concentration (x_c) below which water mobility is highly restricted. Below x_c, *n*PG-water domains drive the dielectric signal whereas above x_c, water-water domains dominate the dielectric response at low temperatures. The results also show that process (II) at low temperatures is due to local motions of water molecules in the glassy frozen matrix. Additionally, we will show that the glass transition temperatures (T_g) for aqueous PG, 2PG, and 3PG solutions do not extrapolate to ~136 K, regardless of the extrapolation method. Instead, we find that the extrapolated T_g value for water from these solutions lies in the neighborhood of 165 K. © *2006 American Institute of Physics*. [DOI: 10.1063/1.2198206]

I. INTRODUCTION

A good glass former is one for which the cooling rate needed to avoid crystallization is low. Typical examples, among others, are glycerol,[1] *o*-terphenyl,[2] and propylene glycol.[3] It is well known that water crystallizes on cooling, making it difficult to study in the supercooled state. A direct consequence is the determination of the glass transition temperature (T_g) of water. One way to avoid the crystallization, both on cooling down from liquid water and on heating up from glassy state, is by mixing water with other liquids or salts. In this case it is possible to avoid crystallization and, by extrapolation, to reveal the properties of supercooled water in the inaccessible temperature range (150–235 K).

The dielectric behavior of aqueous solutions has been extensively studied in the past. Most of these studies were made in the relatively high temperature range (~25 °C), showing the existence of only one process (symmetric or asymmetric depending on the involved liquid).[3–6] Contrary to this behavior, in the low temperature range (150–200 K) aqueous solutions usually show two relaxation processes in the liquid-rich side (water concentrations lower than 50%) as in the case of ethylene-glycol oligomer water mixtures.[7] The relaxation times of the slower process [process (I)] usually follow a Vogel-Fulcher-Tammann (VFT) equation[8] and its origin was related to the α relaxation of the system formed by the solute and the solvent used. On the other hand, the relaxation times for the faster process [process (II)] show an Arrhenius behavior and were associated with the relaxation of the water molecules present in the solutions. Since the consensus for the last two decades has been that T_g for water (i.e., the temperature for which $\tau_\alpha \approx 100$ s) is located at about 136 K,[9,10] process (II) was interpreted as the α relaxation of water molecules. However, this relaxation process has a symmetric shape which is not expected for an α process. Furthermore, the Arrhenius temperature dependence of its relaxation time is consistent with a local process and is very rarely seen for the α relaxation in other glass forming materials. Moreover, in a recent work we have found evidence[11] that the dielectric relaxation process of confined water that has been associated with the long accepted T_g of water (~136 K) must be a local process which is not directly related to the actual glass transition.

Recently, a vigorous controversy has arisen in the scientific literature[12–16] about the true value of the water's glass transition temperature. As mentioned above, the accepted temperature value for water's glass transition during the last decades was 136 K.[9,10] However, Velikov *et al.*[13] have recently analyzed calorimetric data on hyperquenched glassy water. The authors suggest that if the glass transition temperature for water is the accepted value of ~136 K, liquid water would be anomalous compared with other glass forming liquids. Normal behavior is restored if water's glass transition is reassigned to a value in the range of 165–180 K.

Summarizing, two processes usually appear in water so-

[a]Electronic mail: scerveny@sw.ehu.es

lutions but the interpretation of the faster [process (II)] is uncertain. For this reason, we have studied the dielectric behavior of oligomers of propylene glycol (*n*PG, $n=2,3$) water solutions. In particular, we focus on the relaxation seen at low temperatures (150–200 K) [process (II)] on the *n*PG-rich side. Previous studies[17] on propylene glycol (PG) water solutions showed that the structure that water adopts in PG-water solutions is different from the rest of aqueous solutions. It is worth noticing that although propylene glycol has been studied in detail in pure form,[3,18,19] extensions to water solutions at low temperatures have, to the best of our knowledge, never been performed. It is important to note that these results may have a significant impact on our understanding of the behavior of water in contact with biological materials and in microporous materials.

II. EXPERIMENT

Dipropylene glycol (2PG) and tripropylene glycol (3PG) ($H-[OCH(CH_3)CH_2]_n-OH(n=2,3)$) were used in this study to prepare aqueous solutions with different concentrations. 2PG and 3PG were purchased from Aldrich Chemical Company, Inc. and opened and manipulated inside a glovebox under a controlled argon atmosphere. Aqueous *n*PG solutions were prepared varying the water concentration from 0% to 50% (w/w). The bottles with the different solutions were sealed and put in an ultrasonic cleaner for 30 min to ensure a good microdispersion and a homogeneity at molecular level.

A broadband dielectric spectrometer, Novocontrol alpha analyzer, was used to measure the complex dielectric function, $\varepsilon^*(\omega)=\varepsilon'(\omega)-i\varepsilon''(\omega)$, $\omega=2\pi f$, in the frequency (f) range of $10^{-2}-10^6$ Hz. The solutions were placed between parallel gold-plated electrodes with a diameter of 20 mm and three Teflon spacers of 0.1 mm were used to define the thickness. After cooling at a rate of 10 K/min, isothermal frequency scans recording $\varepsilon^*(\omega)$ were performed every 5° over the temperature range of 130–280 K. The sample temperature was controlled with stability better than ±0.1 K.

A differential scanning calorimetry (DSC) Q1000 TA instrument was used in the temperature modulated differential scanning calorimetry (TMDSC) mode. TMDSC experiments were carried out on heating with a temperature amplitude $T_a=0.8$ K, a modulation period of $t_p=60$ s ($\omega=0.105$ rad s^{-1}), and 5 K/min of underlying heating rate. Hermetic aluminum pans were used for all the samples and a helium flow rate of 25 ml/min was used. The sample weights were about 20 mg.

III. RESULTS

A. Calorimetric results

DSC scans showing the heat flow for some representative water contents of 3PG aqueous solutions during heating are given in Fig. 1. Additionally, a cooling scan for the sample with the highest water content ($c_w=50$ wt %) is shown in the same figure. This last curve shows that using this cooling rate no crystallization on cooling occurs in the samples for any water content. Thus, by cooling at 10 K/min fully amorphous material is obtained at low temperatures.

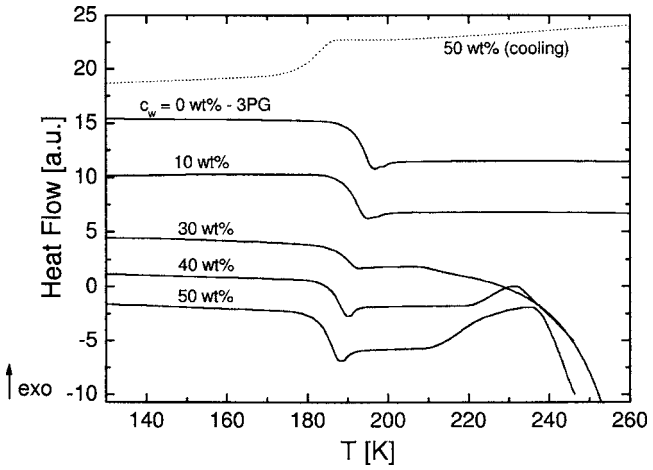

FIG. 1. TMDSC scans of 3PG-water solutions at different water concentrations during heating at a rate of 5 K min^{-1}. The dotted line shows a cooling scan at a rate of 10 K min^{-1} for a sample with $c_w=50$ wt %.

Heating scans in Fig. 1 show two typical temperature regions for *n*PG-water solutions: a glass transition followed by a cold crystallization. Cold crystallization at 10 K/min is observed for high water concentrations ($c_w \geqslant 30$ wt %), whereas it is absent for lower water contents. Similar results were obtained for 2PG-water solutions. Glass transition temperatures for *n*PG-water solutions are shown in Table I.

B. Dielectric results

Typical isotherms representing the dielectric loss, $\varepsilon''(f)$, of 3PG-water mixtures at two different concentrations are shown in Figs. 2 and 3. Similar spectra were obtained for 2PG. Below the solution's glass transition temperature ($T_{g,\mathrm{sol}}$), the isotherms present a wide sub-T_g relaxation. In the vicinity of $T_{g,\mathrm{sol}}$ measured by DSC, isotherms also show the α relaxation of the solutions in the low-frequency range followed by the stronger sub-T_g process in the high-frequency range (see curves at $T=188$ K in Figs. 2 and 3). In this temperature range both contributions to the dielectric loss are well separated in frequency. At higher temperature, two different behaviors were observed depending on the water con-

TABLE I. VFT parameters for process (I) of *n*PG aqueous solutions. $T_{g,\mathrm{sol}}$ indicates the extrapolation of T_g at 100 s whereas T_g DSC indicates the onset of calorimetric T_g.

c_w (wt %)	log τ_0 (s)	T_0 (K)	D	$T_{g,\mathrm{sol}}$ (K)	T_g (DSC) (K)
Pure 3PG	−12.7	150.8	8.7	188.6	191.0
10	−14.3	140.0	12.4	186.3	188.7
20	−14	135.7	13.6	185.8	186.8
30	−14.5	137.2	12.95	184.0	185.9
40	−14.2	140.0	11.5	183.2	185.2
50	−13.9	144.6	9.3	181.3	182.6
Pure 2PG	−12.9	153.0	9.3	194.5	195.4
10	−13.8	138.4	12.5	186.0	188.4
20	−13.7	136.8	12.2	183.0	184.4
30	−14.2	136.1	12.0	180.0	183.1
40	−13.8	138.4	10.6	178.8	182.1
50	−12.8	143.0	7.4	175.0	178.2

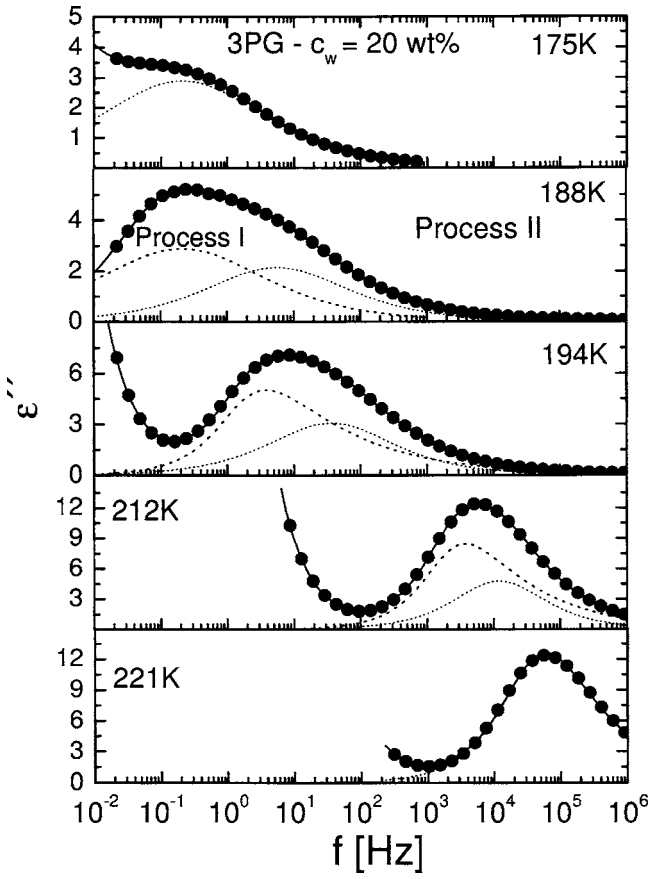

FIG. 2. Loss component ε'' of the complex dielectric permittivity $\varepsilon^*(f)$ of 3PG-water solution with a water concentration of 20 wt % at some representative temperatures. At 188 K an example of the fitting procedure is also included (see text). The solid line through the data points is a least square fit to a superposition of a power law for conductivity, the imaginary part of a Havriliak-Negami function for the process (I), and the imaginary part of a Cole-Cole function for process (II). At 221 K it is possible to observe the merging between processes (I) and (II).

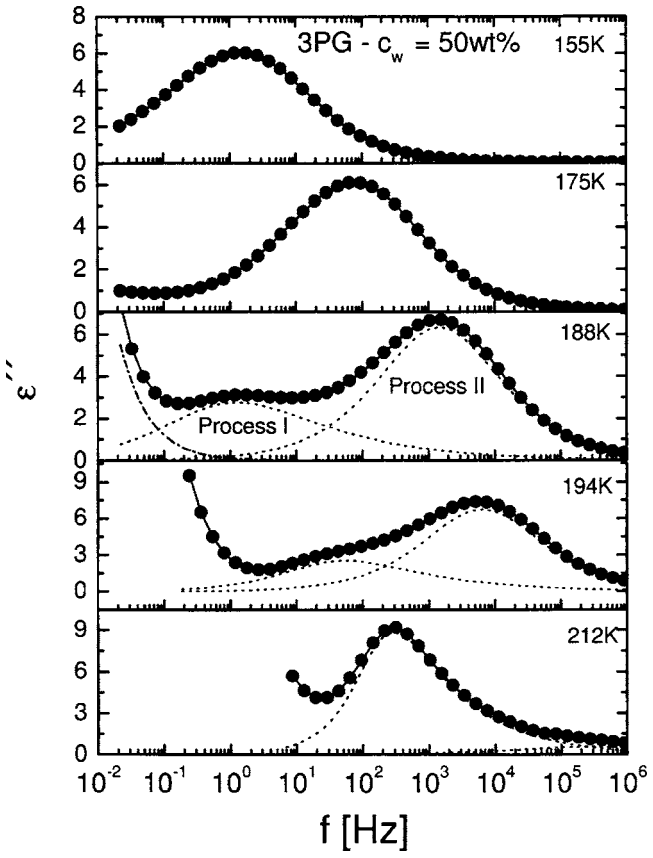

FIG. 3. Loss component ε'' of the complex dielectric permittivity $\varepsilon^*(f)$ of 3PG-water solution with a water concentration of 50 wt % at some representative temperatures. At 188 K an example of the fitting procedure is shown (see text). The solid line through the data points is a least square fit to a superposition of a power law for conductivity, the imaginary part of a Havriliak-Negami function for the process (I), and the imaginary part of a Cole-Cole function for process (II). At 212 K it is possible to observe a change in the dynamics due to water crystallization around this temperature as measured by DSC.

tent in the samples. For water content lower than 30 wt % and in the neighborhood of 220 K (temperatures well above T_g) both relaxations coalesce into a single peak (see Fig. 2 at $T=221$ K). In contrast, for samples at high water content ($c_w \geqslant 40$ wt %), no merging was observed but a change in the behavior of the dielectric spectra was noted at around 206 K (see Fig. 3 at 212 K). This change could be related to the onset of water crystallization.

To analyze the frequency dependence of the complex permittivity, we used the Havriliak-Negami (HN) equation[20]

$$\varepsilon^*(\omega) = \varepsilon_\infty + \frac{\Delta\varepsilon}{[1+(i\omega\tau_{\mathrm{HN}})^\alpha]^\gamma}, \tag{1}$$

where $\Delta\varepsilon=\varepsilon_s-\varepsilon_\infty$, ε_∞ and ε_s being the unrelaxed and relaxed values of the dielectric constant, τ_{HN} is the relaxation time, and ω is the angular frequency. In Eq. (1) α and γ are shape parameters ($0<\alpha,\alpha\gamma\leqslant 1$). By setting $\gamma=1$ a symmetrical function is obtained [Cole-Cole (CC) function[21]] which is widely used to describe secondary relaxations in glassy materials. A markedly asymmetric Cole-Davidson (CD) function[22] is obtained with $\alpha=1$.

An example of the fitting procedure was presented in Figs. 2 and 3 for a 3PG-water solution at 188 K. In the present study we chose a free Havriliak-Negami [Eq. (1)] to fit the α-relaxation data for *n*PG-water solutions whereas the sub-T_g relaxation was described using Eq. (1) with $\gamma=1$ (CC function) for temperatures up to its merging with the α relaxation. At low frequencies conductivity effects dominate and to account for that a power law term was added to the sum of CC and HN functions. It is important to note that for low water content (10 wt %) it is possible to observe a small contribution in the dielectric response from the β relaxation of pure *n*PG [see the corresponding relaxation time in Fig. 4(a)]. The intensity of this process is very small and is screened when more water is added to the mixture. Figures 6(a) and 6(b) show the parameters for this process. In this work we do not consider this small contribution for water content higher than 10 wt %.

C. Relaxation times, shape parameters, and dielectric strength

The obtained relaxation times for bulk 3PG are shown in Fig. 4(a) (open symbols). A typical behavior for a glass forming liquid is observed with one non-Arrhenius α relaxation and one Arrhenius β relaxation. The relaxation map for $c_w=10$ wt % is also shown in the same figure (filled sym-

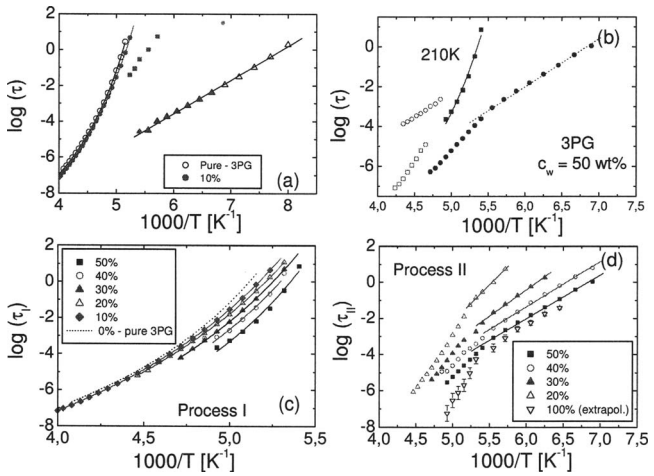

FIG. 4. Plot of the characteristic relaxation times τ for 3PG aqueous solutions. (a) Open circles and triangles are the relaxation times of the α relaxation and β process, respectively, for pure 3PG. For a solution with c_w = 10 wt %, three processes are observed: process (I) (filled circles), process (II) (filled squares), and β relaxation for 3PG (filled triangles). (b) Temperature dependence of τ for c_w=50 wt % [full boxes: main relaxation process (I), full circles: process (II), open circles: relaxation process due to ice, and open squares: the α relaxation of 3PG-water solutions but with a different concentration of water (see text)]. (c) Temperature dependence of τ [process (I)] for 3PG-water solutions. The solid lines are fits of the VFT equation to the data. The dotted curve is the same as the curve shown in (a) for pure 3PG. (d) Relaxation times related to the process (II) for 3PG-water solutions. The results of fitting Arrhenius functions to the data are shown with solid lines. At temperatures higher than the calorimetric T_g, the relaxation times speed up from the Arrhenius behavior.

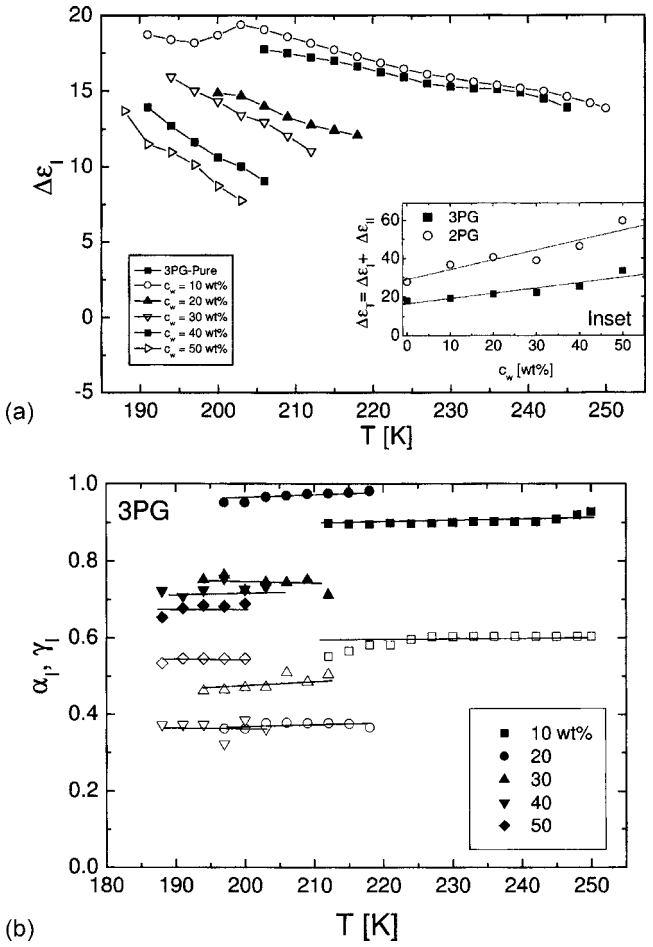

FIG. 5. (a) Temperature dependence of the relaxation strength of process (I), $\Delta\varepsilon_I$ at different water contents for 3PG-water solutions as obtained from the fitting. (b) Shape parameters against temperature for 3PG-water solutions at different concentrations (filled and open symbols represent α and γ parameters, respectively). Inset A: Total relaxation strength $\Delta\varepsilon_T$ vs water concentration at a fixed temperature (T=203 K).

bols). In addition to process (I) (filled circles) and process (II) (filled squares), the relaxation times corresponding to the β relaxation of pure 3PG are observed at this low water content. Figure 4(b) shows the relaxation times for a sample with a water content of 50 wt % as obtained from the analysis described above. The relaxation times of the α relaxation of the solution [process (I)] and the additional faster and stronger process [process (II)], which shows an Arrhenius behavior for temperatures up to $T_{g,\mathrm{sol}}$, exhibit a continuous behavior for temperatures up to 206 K. Above this temperature crystallization appears, as measured by DSC (see Fig. 1), and two different relaxation processes emerge. The slower process is related to the presence of ice in the samples and it was only seen for high water concentrations (40 and 50 wt %), whereas the faster process is the response of the *n*PG-water solution but with a lower water concentration because some of the water has already crystallized. The slower process is similar to that observed by Hayashi *et al.* in glycerol-water mixtures[23] although in that case more water was necessary to observe crystallization (around 80 wt % of water). The temperature at which the splitting occurs (206 K) is the same in these two different materials. In the present work, we restrict our discussion to temperatures lower than 206 K where no crystallization is observed. In Figs. 4(c) and 4(d) we show the temperature dependence for the relaxation times, at different concentrations, for processes (I) and (II), respectively.

A direct inspection of Fig. 4(c) shows that the α process of the solution becomes faster when increasing water content, as usual for other water solutions.[24,25] The temperature dependence of τ_α can be well described by the VFT equation,[8] $\tau_\alpha = \tau_0 \exp(DT_0/T - T_0)$, where τ_0 is the relaxation time in the high temperature limit, T_0 is the temperature where τ_α tends to diverge and is often identified with the Kauzmann temperature, and D parametrizes the departure from Arrhenius behavior and distinguishes between strong and fragile glasses (high and low D, respectively). Extrapolation of this formula to a relaxation time of ~100 s uses to give a dielectric estimation of the glass transition temperature of the solutions, $T_{g,\mathrm{sol}}$. This $T_{g,\mathrm{sol}}$ and the VFT parameters describing the temperature dependence of the α-relaxation times for *n*PG-water solutions are given in Table I. T_g values for the solutions, measured by DSC, are given in the same table. Both values, T_g and $T_{g,\mathrm{sol}}$, are very close to each other and thus we conclude that the dielectric relaxation we are observing [process (I)] is related to the glass transition of the solution. The relaxation strength of this process, $\Delta\varepsilon_I$, as obtained from the fits is shown in Fig. 5. By adding 10 wt % of water, $\Delta\varepsilon_I$ slightly increases and then it is reduced with increasing amount of water.

Turning to the process (II), for temperatures below $T_{g,\mathrm{sol}}$,

TABLE II. Activation energy (E) and preexponential factor [log τ_0 (s)] obtained from the Arrhenius equation applied to the low temperature data [see solid line in Fig. 4(d)] for all the concentrations.

	3PG		2PG	
c_w(wt %)	log τ_0 (s)	E (eV)	log τ_0 (s)	E (eV)
10	⋯	⋯	⋯	⋯
20	−22.5±0.2	0.81±0.01	⋯	⋯
30	−17.9±0.1	0.58±0.01	−18.2±0.1	0.59±0.01
40	−16.4±0.2	0.50±0.01	−16.4±0.2	0.50±0.01
50	−16.4±0.3	0.48±0.01	−15.2±0.3	0.45±0.01

we observe that the relaxation times [see Fig. 4(d)] have an Arrhenius temperature dependence (for temperatures up to $T_{g,\mathrm{sol}}$)

$$\tau(T) = \tau_0 \exp(E/kT), \tag{2}$$

where for a simple activated process τ_0 would correspond to the molecular vibration time and E is the activation energy. The fitted values for E and τ_0 are shown in Table II. Activation energy decreases with increasing water concentration. Note that unphysical low values of τ_0 were obtained more evidently at low water concentrations.

Temperature dependences of the relaxation strength ($\Delta\varepsilon_{\mathrm{II}}=\varepsilon_s-\varepsilon_\infty$) and shape parameter ($\alpha_{\mathrm{II}}$) are shown in Figs. 6(a) and 6(b), respectively. Both parameters are almost temperature independent but greatly affected by the amount of water. A strong increase in $\Delta\varepsilon_{\mathrm{II}}$ is observed for the samples with $c_w \geqslant 20$ wt %. This increase in the relaxation strength cannot come only from the increasing number of relaxing water molecules but it also indicates an increase in the ability of water for reorientation. The total relaxation strength ($\Delta\varepsilon_T=\Delta\varepsilon_{\mathrm{I}}+\Delta\varepsilon_{\mathrm{II}}$), plotted in the inset A of Fig. 5(a) at a fixed temperature, shows that $\Delta\varepsilon_T$ increases with increasing water content as expected because of the high dielectric constant of water. However, the relaxation strength of this process, normalized with the *n*PG content [not shown], remains approximately constant, within the experimental error, at around the same value obtained for 10 wt %.

Finally, above the solution's T_g, the relaxation time of process (II) changes its temperature behavior. There is a systematic reduction of the relaxation times with respect to the extrapolation of the Arrhenius line observed at temperatures lower than $T_{g,\mathrm{sol}}$ and this effect is more pronounced for high water contents [see Fig. 4(d)]. It is important to note that at $T>T_{g,\mathrm{sol}}$ the total dielectric loss spectra were analyzed using a simple superposition of two peaks which is only valid if the two processes [(I) and (II)] are well separated in time.[26] Below T_g, these criteria are fulfilled as the relaxation times of the processes (I) and (II) are separated by more than 6 decades. However, above $T_{g,\mathrm{sol}}$ the time scales of the processes (I) and (II) rapidly become more and more similar and a simple superposition is no longer valid. The observed apparent change in activation energy is a phenomenon that can be explained using Williams's ansatz.[27] The observed relaxation time is at these high temperatures given by an effective relaxation that is due to a convolution of the two processes.

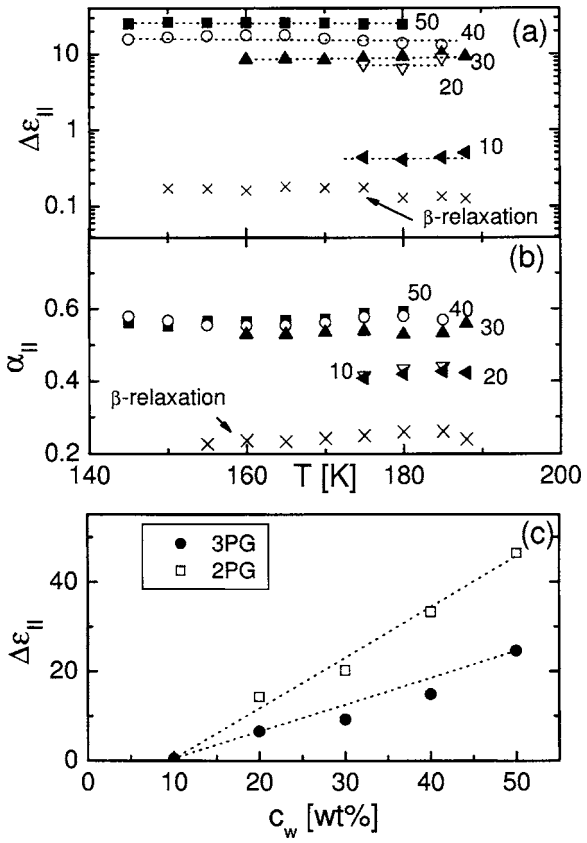

FIG. 6. (a) Temperature dependence of the relaxation strength of process (II), $\Delta\varepsilon_{\mathrm{II}}$ and (b) shape parameter α_{II} at different water contents for 3PG-water solutions as obtained from the fitting. In addition, for low water content (10 wt %), it is possible to observe the β relaxation of pure 3PG (crosses). (c) Variation of $\Delta\varepsilon_{\mathrm{II}}$ with water content for 2PG and 3PG aqueous solutions. $\Delta\varepsilon_{\mathrm{II}}$ is the averaged value taken from (a).

In this sense the relaxation times of process (II) above $T_{g,\mathrm{sol}}$ carry information also about the relaxation time of process (I).

IV. DISCUSSION

The experimental results show two relaxation processes for *n*PG-water mixtures. Process (I) is a manifestation of the global dynamics of the system (global in the sense that both components are involved in this process). In contrast, process (II) is a manifestation of the water dynamics, which is faster than process (I) and it persists at temperatures lower than $T_{g,\mathrm{sol}}$.

A. Global dynamics (α relaxation)

As we mentioned above, process (I) reflects the dynamics of the system formed by both *n*PG and water molecules as evidenced by the fact that dielectric $T_{g,\mathrm{sol}}$ is comparable with the T_g measured by DSC (see Table I). The shape parameters [α and γ in Eq. (1)] are both temperature independent [as shown in Fig. 5(b)], indicating that time-temperature superposition is approximately valid for process (I) up to 206 K where crystallization of water takes place for concentrations higher than 30 wt %. Additionally, it was also ob-

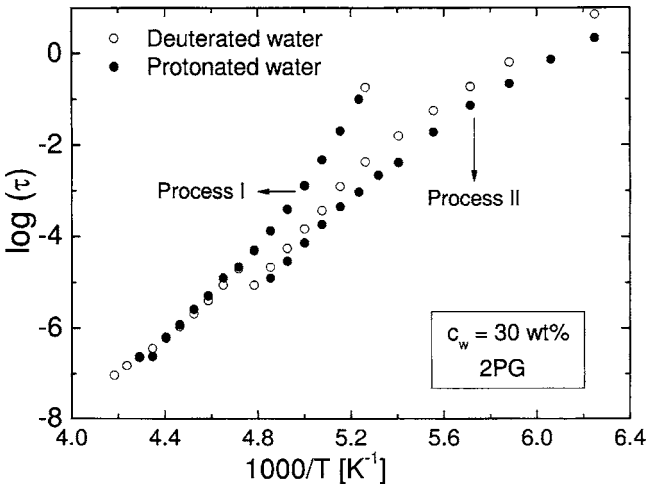

FIG. 7. Comparison between the relaxation times (τ_{max}) for 2PG-deuterated and protonated solutions with a concentration of 30 wt %. Open and filled symbols represent deuterated and protonated samples, respectively.

served that $T_{g,sol}$ decreases as the water content increases, i.e., water facilitates the motion of *n*PG acting like a plasticizer.

B. Process (II): Water dynamics

The main feature of this process is that its strength increases with increasing water content and it persists essentially with the same strength well below the solution T_g [see Fig. 6(a)]. This is contrary to what is observed in conventional glass formers where below T_g most of the dipolar relaxation cannot take place within accessible times. According to our results the dielectric losses of process (II) correspond to relatively large angular reorientations (in the sense that its relaxation strength is of the order of that expected from water molecules that are able to reorientate completely) of water molecules occurring even when the solution is frozen. Although the global structure of the system is basically "frozen," a significant molecular mobility remains in the glassy state. In a conventional glass forming liquid, one expects a less intensive secondary process such as in the case of *o*-terphenyl.[2] However, in the binary liquid studied here the situation appears to be different. Process (II) is more intense than the α relaxation. It thus seems that the dipoles that are relaxing when the solution is frozen are those from water.

To clarify this further, deuterium isotopic substitution was used in one of the samples (c_w=30 wt %). It is commonly assumed that the interactions (hydrogen or deuterium bonds) are not significantly modified by the isotopic substitution. However, because of the higher mass of deuterium compared to hydrogen, the relaxation times should be slower than those in nondeuterated materials. Figure 7 shows the relaxation times for samples containing deuterated (open circles) and normal water (full circles). The characteristic times for the α relaxation are unchanged but process (II) is significantly slower for the deuterated sample. The observed difference in time scale between the two samples is similar to that found in dielectric studies of the isotopic substitution effects on the dielectric relaxation of liquid water performed at high frequencies[28] (in the terahertz range) and high temperatures (270–368 K). Thus, it appears that process (II), below $T_{g,sol}$, is due to the mobility of water molecules in the "local cages"[29,30] created in the glassy solution.

On the other hand, as shown in Fig. 6(c), the composition dependence of the dielectric strength ($\Delta\varepsilon_{II}$) shows an onset at water concentrations of around 10 wt %. The fast increase of $\Delta\varepsilon_{II}$ at higher concentrations would be an indication that the new water molecules start interacting with other water molecules and only a small fraction remains interacting with the *n*PG. This observation would imply that at low water concentrations (around 10 wt %), the mobility of water is highly restricted and that domains of water and *n*PG are present in the samples and the corresponding dipole reorientation would take place only above T_g [i.e., by process (I)]. Thus, at higher concentrations two "types" of water molecules would be present in the samples: water molecules bound to *n*PG and water molecules ("excess water") that likely are not directly linked to *n*PG and present a higher mobility. It is important to note that this structure only would be stable at low temperatures (<250 K) because at higher temperatures water crystallization occurs. Interestingly, in a deep study of dimethyl sulfoxide[31] and ethylene glycol[32] water solutions, Murthy observed the same behavior, although in the last case the complexlike behavior was observed at higher water concentrations. So, it seems that water interacts strongly with several liquids and polymers in the low hydration regime. For instance, some of us studied the hydration of polyvinyl methyl ether[33] and it showed a similar behavior, i.e., the existence of a stable complex for low temperatures or at least at temperatures lower than the solution T_g.

Summarizing, the proposed scenario for *n*PG aqueous solutions at low temperatures ($T<T_{g,sol}$) is that water molecules interacting with *n*PG would govern the dielectric spectra at low water concentrations. However, at higher water concentrations, water-water interactions should allow larger reorientations of the excess water molecules and thereby give a major contribution to the total dielectric response. In agreement with this idea, the symmetric broadening of the relaxation process of water decreases with increasing water content. At $c_w \leqslant 30$ wt %, the relaxation is very broad, thus indicating multiplicities of local environments for the water molecules that contribute to the dielectric signal. As the water content increases the dielectric response becomes narrower and this is indicative of a more homogeneous environment (water surrounded by water). We also note that, in this view, the dynamics of the *n*PG-water mixtures evokes the dynamic of water near a protein surface:[34] one part of the water is bound to *n*PG and the other one is not directly interacting with it and would behave essentially like bulk water.

Turning to the concentration dependence of the relaxation times for process (II), Fig. 4(d) shows that they become faster with increasing water content. The time scales of the relaxation process of H-bond liquids (water, alcohols, or their mixtures) are generally associated with the probability that molecules in the system find a new H-bond partner.[35–37] The reason for the relaxation times to be faster for high water content could be that water molecules contribute with more

H-bond sites per volume unit than the *n*PG molecules. Thus, as the water content increases the available H-bond sites per volume unit also increase and therefore the breaking and reforming of H bonds become more probable.

All the discussion above concerns the behavior of process (II) at temperatures below the glass transition of the solution. However, as mentioned above, at high temperatures the relaxation times deviate from the low-T Arrhenius behavior and this deviation is more pronounced at high water content. A way to explain such features is to consider that when the binary liquid reached the solution's T_g the mobility of the matrix increases and the local cages confining the mobile water molecules at low T disappear. This would increase the probability for H-bond interchange and the mobility of the water molecules will approach that of supercooled water. This can be mathematically explained using Williams's ansatz, as discussed above.

If the scenario given above is correct, we have a way to extrapolate the relaxation times to 100% of water. To do this, we plotted for each temperature the relaxation time data of 3PG solutions as a function of concentration. Due to the lack of an appropriate frame to extrapolate the relaxation times at 100% of water, we used an empirical single exponential function to calculate the extrapolated values. The result of such procedure is given in Fig. 4(d) (open inverted triangles). The extrapolation was made for the whole temperature range (from 155 to 206 K) but it is important to make clear that two different behaviors of water are displayed in the figure; at $T<185$ K water is confined by the glassy matrix (and no cooperative motions are observed). At $T>190$ K, when the system allows for the formation of more extended hydrogen bonded water network (which is required for the cooperative α relaxation to be observed), water molecules are able to relax in a cooperative way. Although the first impression is that relaxation times, both at low and high temperatures, define a single relaxation process this is not correct since in this case water is in different conditions (confined and bulklike). Note that ethylene glycol-water mixtures[7] also show the same deviation from the Arrhenius behavior when the solution reaches its $T_{g,\mathrm{sol}}$.

The extrapolated values for bulklike water are shown again in Fig. 8 (open and filled circles) together with relaxation times for bulk liquid water measured by dielectric spectroscopy[28] (filled triangles) above its melting point. The shadow area in the figure divides the two different behaviors. In the low temperature region extrapolated values for confined water are shown by open circles whereas at high temperature extrapolated data are shown by full circles. Thus, at high temperatures ($T>185$ K), the relaxation time shows how water behaves like a fragile supercooled liquid up to room temperature.

The temperature dependence of the relaxation times, by taking both the extrapolated values and those measured close to room temperature (filled circles and triangles, respectively, in Fig. 8), was fitted with a VFT equation. The best fit of the experimental data was obtained with $\log(\tau_0)=-13.1$, $T_0=156.8$ K, and $D=4.06$; the corresponding curve is shown in Fig. 8 (dashed line). The extrapolated glass transition temperature at 100 s for this process is around 175 K. Although

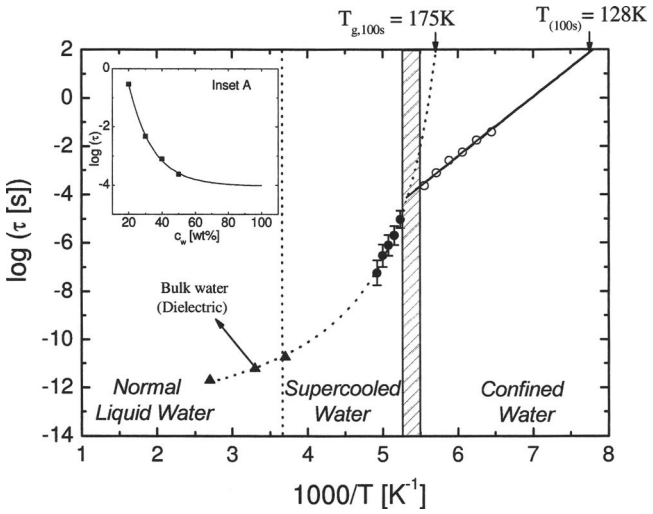

FIG. 8. Relaxation map for extrapolation to 100 wt % of water. Open and filled circles represent the extrapolated relaxation times to 100 wt % of water. Filled triangles represent the relaxation times of bulk water measured by dielectric spectroscopy above its melting point (Ref. 28). Solid line is the best Arrhenius fit to the low temperature data. Dashed line represents the VFT behavior of the relaxation time for normal and supercooled water. The extrapolation within the dashed area is not possible because the transition temperature between Arrhenius and VFT behaviors is concentration dependent. Inset A: Relaxation times as a function of concentration for 3PG-water solutions at $T=185$ K. The line represents the extrapolation to 100 wt % (see text).

this value is subjected to a rather high uncertainty, the lowest T_g values compatible with the extrapolated relaxation time data would be around 160 K (calculated using an Arrhenius equation). Thus, the findings are consistent with a T_g of water at a higher temperature ($\approx$160–180 K) as suggested by Angell[12] and Velikov *et al.*[13] There is, however, no evidence from this analysis that supercooled water undergoes a strong-fragile transition at around 228 K as has been earlier proposed.[38]

The symmetric shape of the peak at low temperatures, together with the Arrhenius character of the relaxation times, is fully consistent with a local process (β-like process). In addition, no calorimetric event was observed in this low temperature range. So, process (II) at low temperatures is rather due to a local water relaxation than its α relaxation.

Figure 4(c) shows that $T_{g,\mathrm{sol}}$ decreases with increasing water content as usual for such mixtures. Different aqueous solutions have been used to extrapolate the T_g value of the solution to that of the pure water. For instance, Sare and Angell[39] showed that the glass transition temperature predicted by extrapolation of binary solution data on many salt + water systems was consistent with the commonly accepted value of ~136 K for the water glass transition; this was subsequently supported by extrapolation involving a number of molecular liquids.[40] The most important limitation of this method is that for high water contents crystallization starts appearing. An extrapolation can also be done from high *n*PG content values to that of pure water. Figure 9 shows the T_g values of the solutions versus the *n*PG content (PG values were taken from Ref. 11). The solid line in Fig. 9 represents the best fit of the experimental data to the well-known Gordon-Taylor equation[41]

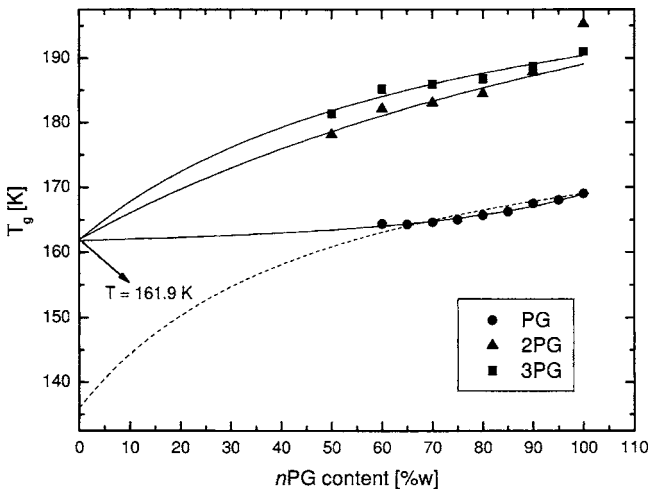

FIG. 9. Glass transition temperature vs *n*PG content for *n*PG aqueous solutions. The lines represent the best fit of the experimental data with Eq. (3). The extrapolations suggest a value of 162±1 K for the glass transition of pure water. Note that an extrapolation to the commonly accepted T_g =136 K seems unphysical (dashed line).

$$T_g(x) = \frac{T_{g1}x + T_{g2}k(1-x)}{[x + k(1-x)]}, \tag{3}$$

where T_{g1} and T_{g2} are the *n*PG and water glass transition temperatures, respectively, x is the *n*PG content, and k is the interaction parameter. The fitting procedure was done by fixing T_{g1} to *n*PG glass transition temperature (except for 2PG whose T_g is anomalously high) and leaving T_{g2} and k as free parameters. A value of 162±1 K for the water's glass transition was obtained. The obtained value for the water's T_g is significantly above the old accepted value of ~136 K, in agreement with the newly suggested value based on thermodynamic considerations.[13] This is also consistent with the dielectric findings discussed before and showed in Fig. 8.

V. CONCLUSIONS

The dielectric results of *n*PG-water solutions show two clear relaxation processes; the faster one related to the water molecules and the slower one due to the α relaxation of the water-*n*PG solution. In addition, from the faster process we found that two different types of water are present in the mixtures. Up to a concentration of around 10 wt % water is mainly bounded to *n*PG. For higher water concentrations the "excess water" dominates the dielectric response. Additionally, two different environments for water molecules are present in the samples. At temperatures lower than $T_{g,\mathrm{sol}}$, water is confined in the glassy matrix formed by *n*PG and water itself, showing an Arrhenius behavior of the relaxation times. At higher temperatures, when the mobility of the matrix increases, water is able to form an extended network and relax in a cooperative way. Thus water behaves like confined water at $T < T_{g,\mathrm{sol}}$ and like bulk water for temperatures above $T_{g,\mathrm{sol}}$ where a departure from the Arrhenius behavior is observed. Finally, a value in the neighborhood of 160–170 K was obtained for the glass transition of pure water by extrapolating the glass transition temperatures obtained by DSC. This result is compatible with the extrapolation of the relaxation times at 100 s measured by dielectric spectroscopy.

ACKNOWLEDGMENTS

Three of the authors (S.C., G.A.S., and A.A.) acknowledge the support of the University of Basque Country and the Basque Government: Project No. UPV/EHU, 00206.215 13568/2001 and the Spanish Ministry of Education Project No. MAT2004-01017. Another author (J.S.) is a Royal Swedish Academy of Sciences Research fellow supported by a grant from Kunt and Alice Wallenberg Foundation. The Swedish Research Council and the Swedish Foundation for Strategic Research are also acknowledged for financial support.

[1] C. A. Angell, J. Non-Cryst. Solids **13**, 131 (1991).
[2] L. Wu and S. R. Nagel, Phys. Rev. B **46**, 11198 (1992).
[3] C. A. Angell, L. Böhm, M. Oguni, and D. L. Smith, J. Mol. Liq. **56**, 275 (1993).
[4] N. Shinyashiki, S. Sudo, W. Abe, and S. Yagihara, J. Chem. Phys. **109**, 9843 (1998).
[5] R. J. Sengwa, R. Chaudhary, and S. C. Mehrotra, Mol. Phys. **99**, 1805 (2001).
[6] S. Sudo, N. Shinyashiki, Y. Kitsuki, and S. Yagihara, J. Phys. Chem. A **106**, 458 (2002).
[7] S. Sudo, S. Tsubotani, M. Shimomura, N. Shinyashiki, and S. Yagihara, J. Chem. Phys. **121**, 7332 (2004).
[8] H. Vogel, Phys. Z. **22**, 645 (1921); G. S. Fulcher, J. Am. Chem. Soc. **8**, 339 (1925); **8**, 789 (1925); G. Tammann and W. Hesse, Z. Anorg. Allg. Chem. **156**, 245 (1926).
[9] P. G. Debenedetti, *Metastable Liquids* (Princeton University Press, Princeton, NJ, 1996).
[10] G. P. Johari, A. Hallbrucker, and E. Mayer, Nature (London) **330**, 552 (1987).
[11] S. Cerveny, G. A. Schwartz, R. Bergman, and J. Swenson, Phys. Rev. Lett. **93**, 245702 (2004).
[12] C. A. Angell, Chem. Rev. (Washington, D.C.) **102**, 2627 (2002).
[13] V. Velikov, S. Borick, and C. A. Angell, Science **294**, 2335 (2001).
[14] G. P. Johari, J. Chem. Phys. **116**, 8067 (2002).
[15] N. Giovambattista, C. A. Angell, F. Sciortino, and H. E. Stanley, Phys. Rev. Lett. **93**, 047801 (2004).
[16] G. P. Johari, J. Chem. Phys. **119**, 2935 (2003).
[17] A. Minoguchi, R. Richter, and C. A. Angell, J. Phys. Chem. B **108**, 19825 (2004).
[18] R. Casalini and C. M. Roland, J. Chem. Phys. **119**, 11951 (2003).
[19] J. Swenson, G. A. Schwartz, R. Bergman, and W. S. Howells, Eur. Phys. J. E **12**, 179 (2003).
[20] S. Havriliak and S. Negami, Polymer **8**, 161 (1967).
[21] R. H. Cole and K. S. Cole, J. Chem. Phys. **10**, 98 (1942).
[22] D. W. Davidson and R. H. Cole, J. Chem. Phys. **19**, 1484 (1951).
[23] Y. Hayashi, A. Puzenko, I. Balin, Y. E. Ryaboy, and Y. Feldman, J. Phys. Chem. B **109**, 9174 (2005).
[24] A. Puzenko, Y. Hayashi, Y. E. Ryabov, I. Balin, Y. Feldman, U. Kaatze, and R. Behrends, J. Phys. Chem. B **109**, 6031 (2005).
[25] T. Sato and R. Buchner, J. Phys. Chem. A **108**, 5007 (2004).
[26] R. Bergman and C. Svanberg, Phys. Rev. E **72**, 043501 (2005).
[27] G. Williams, Adv. Polym. Sci. **33**, 60 (1979).
[28] C. Rønne, P. O. Åstrand, and S. R. Keiding, Phys. Rev. Lett. **82**, 2888 (1999).
[29] A. Latz, J. Phys.: Condens. Matter **12**, 6353 (2000).
[30] F. Sciortino, P. Gallo, P. Tartaglia, and S. H. Chen, Phys. Rev. E **54**, 6331 (1996).
[31] S. S. N. Murthy, J. Phys. Chem. B **101**, 6043 (1997).

[32] S. S. N. Murthy, J. Phys. Chem. B **104**, 6955 (2000).
[33] S. Cerveny, J. Colmenero, and A. Alegría, Macromolecules **38**, 7056 (2005).
[34] S. M. Bhattacharyya, Z. G. Wang, and A. H. Zewail, J. Phys. Chem. B **107**, 13218 (2003).
[35] I. Ohmine and S. Saito, Acc. Chem. Res. **32**, 741 (1999).
[36] M. A. Floriano and C. A. Angell, J. Chem. Phys. **91**, 2537 (1989).
[37] J. Barthel, K. Bachhuber, R. Buchner, and H. Hetzenauer, Chem. Phys. Lett. **165**, 369 (1990).
[38] K. Ito, C. T. Moynihan, and C. A. Angel, Nature (London) **398**, 492 (1999).
[39] E. J. Sare and C. A. Angell, J. Solution Chem. **2**, 53 (1973).
[40] D. R. MacFarlane and C. A. Angell, J. Phys. Chem. **88**, 759 (1984).
[41] M. Gordon and J. S. Taylor, J. Appl. Chem. **2**, 493 (1953).